



# Density distribution across the Alpine lithosphere constrained by 3D gravity modelling and relation to seismicity and deformation

Cameron Spooner<sup>1,2</sup>, Magdalena Scheck-Wenderoth<sup>1,3</sup>, Hans-Jürgen Götze<sup>4</sup>, Jörg Ebbing<sup>4</sup>, György Hetényi<sup>5</sup>

5 <sup>1</sup>GFZ German Research Centre for Geosciences, Potsdam, Germany

<sup>2</sup>Institute of Earth and Environmental Science, Potsdam University, Potsdam, Germany

<sup>3</sup>Department of Geology, Geochemistry of Petroleum and Coal, RWTH Aachen University, Aachen, Germany

<sup>4</sup>Institute of Geosciences, Christian-Albrechts-University Kiel, Kiel, Germany

<sup>5</sup>Institute of Earth Sciences, University of Lausanne, Lausanne, Switzerland

10

Correspondence to: Cameron Spooner (spooner@gfz-potsdam.de)

**Abstract.** The Alpine Orogen formed as a result of the collision between the Adriatic and European plates. Significant crustal heterogeneity exists within the region due to the long history of interplay between these plates, other continental and oceanic blocks in the region, and inherited crustal features from earlier orogenys. Deformation relating to the collision continues to the present day. Here, a seismically constrained, 3D, structural and density model of the lithosphere of the Alps and their respective forelands, derived from integrating numerous geoscientific datasets, was adjusted to match the observed gravity field. It is shown that the distribution of seismicity and deformation within the region correlates strongly to thickness and density changes within the crust, and that the present day Adriatic crust is both thinner and denser (22.5 km, 2800 kg/m<sup>3</sup>) than the European crust (27.5km, 2750 kg/m<sup>3</sup>). Alpine crust derived from each respective plate is found to show the same trend with zones of Adriatic provenance (Austro-Alpine and Southern Alps) found to be denser and those of European provenance (Helvetic Zone and Tauern Window) to be less dense, suggesting the respective plates and related terrains had similar crustal properties to the present day prior to orogenesis. The model generated here is available for open access use to further discussions about the crust within the region.

15  
20

## 1 Introduction

The Alps are one of the best studied mountain ranges in the world, yet significant unknowns remain regarding their crustal structure and any links that may exist between the localisation of deformation and seismicity in the region and crustal heterogeneity. Significant amounts of seismicity and deformation within the region correspond to plate dynamics, such as at the convergence of the European and Adriatic plates in North-East Italy (Restivo et al., 2016) where the Adriatic plate is observed to act as a rigid indenter, moving northwards and rotating counter-clockwise into the weaker European plate (Nocquet and Calais, 2004; Vrabec and Fodor, 2006). However, numerous large historic seismic events (Fäh et al., 2011; Stucchi et al., 2012; Grünthal et al., 2013), such as the Magnitude 6.6 Basel earthquake in 1356 AD, lie substantially intra-plate in areas with

25  
30





low amounts of horizontal surface strain (Sánchez et al., 2018) suggesting that features within the crust are also significant factors to their localisation.

Crustal heterogeneities on the European plate, constituting the northern foreland of the Alps, principally derive from different terranes that collided during the Carboniferous age Variscan orogeny (Franke, 2000). Collision during orogenesis resulted in the juxtaposition of crustal domains with differing properties next to one another, such as **Moldanubia and Saxothuringia**, (Babuška and Plomerová, 1992; Freyemark et al., 2016) and also resulted in the creation of the Vosges, Black Forest and Bohemian massifs.

As a consequence of the collision of the Adriatic plate with the European plate from the Cretaceous until the present (Handy et al., 2010), heterogeneity within the Alpine orogen is also very pronounced, however differing interpretations exist on the plate provenance of some features. Traditionally, the Alps have been split into distinct zones according to their plate of origin and metamorphic history, such as the Adriatic derived Austro-Alpine and Southern Alps, the European derived Helvetic Alps and the Penninic zone representing distal margin units and slivers of oceanic crust (Schmid et al., 1989). The Briançonnais crustal block that lies within the Penninic zone derives from the **Iberian plate** (Frisch, 1979). Newer works examining the plate provenance of Alpine zones have reinterpreted some features such as the Tauern Window from Penninic origin to European plate origin (Schmid et al., 2004).

Density distribution throughout the crust of the region is also affected by mantle features and regions of thinned crust resulting in sedimentary depocentres. The crust is thinned at three main depocentres within the region, the Po Basin of the southern foreland, the Molasse Basin of the northern foreland and the Upper Rhine Graben, also within the northern foreland, that formed as part of the European Cenozoic Rift System in the Eocene (Dèzes et al., 2004). Anomalously high densities within the crust are present in the Western Alps, within the Ivrea Zone, as a result of a South East dipping mantle wedge, where mantle and lower crustal rocks are present at upper crustal depths (Zingg et al., 1990) and even at the surface (Pistone et al., 2017 and therein).

Previous published interpretations of crustal features within the orogen have been primarily based upon 2D seismic sections (e.g Brückl et al., 2007), tending to result in simplistic models. However, significant lateral differences in crustal structure have been demonstrated, through the deployment of parallel seismological profiles, spaced 15 km apart in the Eastern Alps (Hetényi et al. 2018), indicating the need for more complex models. Studies that have integrated multiple geo-scientific datasets to create 3D models of the region, have either focussed on smaller sub-sections of the Alps (Ebbing, 2002) or included the Alps as part of a much larger study area (E.g. Tesauero et al., 2008). Therefore the generation of a 3D, crustal scale, gravity constrained, structural model of the Alps and their forelands at an appropriate resolution could be used to more accurately describe crustal heterogeneity in the region. The generation of such an Alpine-wide specific model is made possible by the existence of seismological results from numerous published deep seismic surveys that have been completed throughout the region and available high quality global gravity field models. Within this current work, such data is integrated to give insights into the distribution of densities within the crust as constrained by 3D gravity modelling across the vast majority of the Alpine



65 region and its forelands for the first time, so that questions about the relationship between the distribution of densities within  
the crust and seismicity and deformation patterns can be answered.

## 2 Input Data

Existing geological and geophysical observations from previous published works of the Alps and their respective forelands  
were used as constraints for the generation of the 3D structural model. Topography and bathymetry were utilised unaltered  
from ETOPO1 (Amante and Eakins, 2009), as show in Fig. 1a. The data integrated for the constraint of sub-surface lithospheric  
70 features is shown in Fig. 1b and includes: regional scale, gravitationally and seismically constrained models of the TRANSALP  
study area (Ebbing, 2002), the Molasse Basin (Przybycin et al., 2014) and the Upper Rhine Graben (Freyemark et al., 2017);  
regional scale, seismically constrained models of the Po Basin, such as MAMBo (Turrini at al., 2014; Molinari et al., 2015);  
and seismic reflection heights and their associated P wave velocity from projects such as ALP'75, EGT'86, TRANSALP, ALP  
2002 and EASI (IESG, 1978; IESG & ETH Zuerich, 1981; Ströbenreuther 1982; Mechie et al 1983; Zucca 1984; Gajewski &  
75 Prodehl 1985; Deichmann et al., 1986; Gajewski et al 1987; Gajewski & Prodehl 1987; Yan and Mechie 1989; Zeis et al 1990;  
Aichroth et al 1992; Guterch et al 1994; Ye et al 1995; Scarascia and Cassinis, 1997; Enderle et al 1998; Bleibinhaus &  
Gebrande, 2006; Brueckl et al., 2007; Hetényi et al., 2018). The top surface of the asthenospheric mantle (LAB) was utilised  
unaltered from Geissler (2010).

~~Input data coverage for the constraint of~~ most sub-surface lithospheric features was sufficient however thicknesses of  
80 unconsolidated sediments were not available across the full modelled region. In regions of less dense data coverage,  
continental scale, seismically constrained, integrative best fit models, EuCRUST-07 and EPcrust (Tesauro et al., 2008;  
Molinari and Morelli, 2011) were used in addition. Both models provided complete coverage of major structural interfaces  
and P wave velocities over the whole modelled area at a coarse resolution. Detailed values of unconsolidated sediment  
thicknesses were only available in the Upper Rhine Graben, the Molasse Basin and the Po Basin, as the seismic sections utilised  
85 lacked the resolution for shallower features and the continental scale models did not differentiate between sedimentary strata.  
The free-air anomaly utilised was calculated from the global gravity model EIGEN-6C4 (Förste et al., 2014), at a fixed height  
of 6 km above the datum (Fig. 2, further referred to as observed gravity). As the gravity data source is a hybrid, terrestrial and  
satellite dataset, the potential exists for it to be lacking some of the short wavelength response that a fully terrestrial dataset  
would possess. The fixed height of 6 km was utilised to account for this, so that the vertical component of the gravity response  
90 from the generated structural model (further referred to as calculated gravity) and observed gravity can be directly compared  
during the gravity modelling process.

## 3 Method

Data from numerous existing geoscientific datasets (see Input Data section) were integrated to create a gravity constrained,  
3D, structural and density model of the lithosphere of the Alps and their respective forelands. The study area of this work,  
95 indicated in both Figs. 1a and b, covers a region of 660 km x 620 km where the highest density of data source coverage was



available. The vast majority of the Alps and their forelands are included, with the Central and Eastern Alps and the Northern Foreland the best covered regions.

The software package Petrel (Schlumberger, 1998) was utilised for the creation and visualisation of the modelled surfaces in 3D, representing the key structural and density contrasts within the region. These surfaces were: 1. top water; 2. top unconsolidated sediments; 3. top consolidated sediments; 4. top upper crust; 5. top lower crust; 6. top lithospheric mantle; 7. top asthenospheric mantle. All surfaces were generated with a grid resolution of 20 km x 20 km using Petrel's convergent interpolation algorithm.

Layers of the model were generated by correlation and integration between data sources, with the exception of the following: 1. The water layer was generated from cropping ETOPO1 to 0 m a.s.l. No freshwater bodies were added as they are too small to be of impact at the model resolution utilised; 2. The top unconsolidated sediment surface used in the modelling corresponds to topography and bathymetry, which is plotted in Fig. 1a; 3. As a result of unconsolidated sediment thicknesses from the data sources only being present in the Upper Rhine Graben, the Molasse Basin and the Po Basin, outside of these regions a thickness of 0 was used. This was deemed acceptable due to the lack of unconsolidated sediment thicknesses large enough to be of impact at the model resolution utilised, outside of these regions; 4. The LAB was utilised unedited from the data source as it does not represent a significant density contrast and was therefore deemed sufficient to utilise a lower resolution existing model. Alpine nappe stacks were included within the consolidated sediments layer of the model.

During correlation and integration, a hierarchy of data source types was used and in the case of contradiction between the different data sources those of the highest hierarchy were taken. The hierarchy was derived from the quality, resolution and consistency of data sources and was as follows: 1. regional scale, gravitationally and seismically constrained models; 2. regional scale, seismically constrained models; 3. individual seismic reflection surfaces and interpreted sections; 4. continental scale, seismically constrained, integrative best fit models.

No subduction interfaces were modelled, which was deemed acceptable as multiple studies within the region have shown that the effect of different subduction polarities as well as the presence or lack of subducting plates is small. Previous 2D gravity modelling work across the TRANSALP profile has demonstrated that the differences in gravity response between a model of both different subduction polarities and a model setup with no subducted crust were marginal (Deutsch, 2014). Work into the contribution of subducting slabs in the region to the gravity field have also shown that their impact is also relatively small, in the region of 30 mGal (Lowe, 2019).

The 3D gravity modelling software used for constraining the generated structural model was IGMAS+ (Schmidt et al., 2010), which operates by creating triangulated meshes between points on input surfaces and vertical parallel planes, around a body of homogenous density, to calculate their volumetric contribution to the gravity response. Gravity in the model was calculated at 6 km above the datum to be concurrent with the observed gravity. By doing so the short wavelength response of the calculated gravity was not overestimated as mentioned prior. The top of the model was also set to a height of 6 km with a density of 0 used to represent the column of air between it and topography. The model was set up with a plane spacing of 20 km and constant 20 km spaced points from the correlated input surfaces, resulting in a model grid of 20 km x 20 km horizontal



130 resolution. To account for the edge effect of the gravity field, the model was extended by 50% (330 km) in all directions of the studied area using the surfaces from EuCrust-07 (Tesauro et al., 2008).

The Free Air gravity response was ~~utilised as~~ this work is focussed on the crustal composition of the Alpine region and as up to 4.8km of crust lies above sea level within the modelled area, removing this from the gravity signal was deemed unacceptable. Additionally, the complex geological ~~makeup~~ of the Alps ~~means~~ that the removal of Alpine topography as a Bouguer slab of  
135 homogenous density potentially introduces errors.

The process of gravity modelling ~~utilised~~ the alteration of an initial 3D structural model, comprising surface heights and densities, such that through multiple iterations the resulting model produced a ~~similar~~ gravity field to ~~that of~~ the observed ~~gravity~~. Best practice of such an iterative process allows only one input parameter, density or surface heights, to be altered. Here, the surfaces generated as part of the integration work were ~~used unaltered~~ during the gravity modelling ~~phase~~ as they  
140 were ~~deemed to be~~ better constrained than the densities ~~from the input data~~, leaving only density as a free parameter.

For the calculation of the densities used in the initial structural model, P wave velocities from seismic data sources were converted using the experimentally derived empirical relationship detailed in Brocher (2005). In the absence of seismic data, P wave velocities from the continent ~~scale~~ models listed in the ~~Data Sources~~ section were used to supplement, giving coverage over the entire study area. ~~The water layer was assumed to be a density of 1025 kg/m<sup>2</sup> and the asthenospheric mantle layer~~  
145 ~~3320 kg/m<sup>2</sup>.~~

The densities derived from the P wave velocity conversions were then used in conjunction with densities from the input regional scale, gravitationally and seismically constrained models, to split the layers of the generated model laterally into domains of different density, to reflect the heterogeneous nature of the crust within the region. During the generation of the model, preference was given to ~~resolving~~ major densities contrasts. ~~This involved cases of grouping~~ units of known differing  
150 lithology, age and/or provenance ~~together, should they appear to have a similar density so as~~ to best fit the gravity in the region. An overview of ~~all the mean densities of each density body of the model,~~ derived from the seismic P wave velocities, is ~~found~~ in Table 1.

To ~~identify~~ how well the structural model ~~created~~ fits the gravity field in the region, the calculated gravity was ~~then taken away~~ from observed gravity during interactive ~~alterations~~ of the location of different domains within each layer and their densities,  
155 and the result (further referred to as residual anomaly) interrogated. No filtering for specific wavelengths was done during gravity modelling, with the full signal ~~utilised at all times~~. No presumptions were made ~~over~~ which tectonic features would require domains of different density, with their location ultimately derived from the gravity modelling process.

In the case of anomalies in the residual gravity field, the depth of the source was estimated to be half the width of the anomaly wavelength and the density of the body lying at that depth was increased for a positive residual anomaly or decreased for a  
160 negative residual anomaly. Successive iterations of the model were then generated by modifying the distribution of densities within the model layers. This was repeated until a 3D structural density model of the region was obtained, that best reproduces the indications of both the seismic data sources and the gravity field.



#### 4 Results

Figure 3 shows a North-South cross section through the generated model illustrating the thickness of all main structural layers of the model, the density domains defined within them and the calculated and observed gravity of the section. The location of the cross section can be seen in Fig. 1a but is also marked on all figures illustrating the setup of the model.

Key features noted from the setup of the model indicate more heterogeneity is required in the crust, than in other model layers, to replicate the gravity field and that significant differences exist between the crust of the **European and Adriatic plates**. Sedimentary thicknesses, both unconsolidated and consolidated, are thinner in the Molasse Basin than in the Po Basin and crustal densities and thicknesses can also be observed to differ between the plates. In the orogen itself, the result of incorporating all Alpine nappes within the consolidated sediment layer can be observed, with higher thicknesses in the **central Alps**. The **crust** is thickest below the **central Alps** and is compensated for by a higher thickness and density of the lower crust. The observed gravity along with the calculated gravity of the model can also be observed, indicating a close fit.

Figure 4 shows the thicknesses of the layers of the generated model that were created as a result of the correlation and integration work, with the areal extent of all utilised density domains superimposed on top. An overview of all the final density of all bodies in the model required to fit the gravity field can be found in Table 1.

Both sedimentary layers of the model in Fig. 4 reflect trends across the region previously identified in the Fig. 3 cross sections, with thicker and denser sediments in the Po Basin than in the Molasse Basin, and large thicknesses of consolidated sediments in the central Alps (18 km) representing the Alpine nappe stacks. Maximum thicknesses of 9 km and 12 km were modelled in the Po Basin for unconsolidated and consolidated sediments respectively, whilst 6 km and 9 km were modelled in the Molasse Basin. Thicknesses of 3.75 km unconsolidated sediments were modelled in the deepest part of the Upper Rhine Graben with consolidated sediments of up to 3 km. In both of the modelled sedimentary layers separate density domains were necessary in the Eastern Molasse Basin (2470 kg/m<sup>3</sup> and 2680 kg/m<sup>3</sup>) and the Po Basin (2470 kg/m<sup>3</sup> and 2700 kg/m<sup>3</sup>) that were denser than the sediments in the rest of the region (2450 kg/m<sup>3</sup> and 2670 kg/m<sup>3</sup>).

The modelled configuration of the **European upper crust** is thicker but a similar density on average (20 km and 2700 kg/m<sup>3</sup>), compared to the **Adriatic upper crust** (12 km and 2700 kg/m<sup>3</sup>). The thickest regions of upper crust can be found around the Bohemian massif in the northern foreland and the Briançonnais Terrain and Tauern Window in the Alps at up to 30 km thick, whilst thinned upper crust is modelled below the **Adriatic Sea** and the Ivrea Zone at only 4 km thick. Multiple density domains in the upper crust correspond to known tectonic features in the modelled region such as the Variscan domains of Saxothuringia (2670 kg/m<sup>3</sup>) and Moldanubia (2700 kg/m<sup>3</sup>), the massifs of Bohemia (2740 kg/m<sup>3</sup>) and Vosges/Black Forest (2660 kg/m<sup>3</sup>) that lie close enough together in the model to be grouped, the Ivrea Body (2790 kg/m<sup>3</sup>) and the Apennine plate (2720 kg/m<sup>3</sup>). However, in the Alps and the Adriatic Sea the density domain boundaries modelled were found not to correspond to specific tectonic features. The Alps are divided roughly North East (2740 kg/m<sup>3</sup>) to South West (2670 kg/m<sup>3</sup>), denser in the NE and the Adriatic Sea is split roughly North (2660 kg/m<sup>3</sup>) to South (2700 kg/m<sup>3</sup>), denser in the south.



195 The modelled configuration of the European lower crust is of similar thickness, but less dense on average (10 km and 2860  
kg/m<sup>3</sup>) compared to the Adriatic (10 km and 2910 kg/m<sup>3</sup>). It was found necessary to model the lower crustal Alpine root  
thicker and denser (2950 kg/m<sup>3</sup> and 34 km) than the rest of the region. Density domains within the lower crust correspond less  
with known tectonic features than those in the upper crust. Of the domains in the lower crust only two correspond roughly to  
tectonic features, one to the Saxothuringian Variscan domain (2920 kg/m<sup>3</sup>) and one to the Ivrea Body (3100 kg/m<sup>3</sup>). A large  
200 region of similar density within the lower crust exists, mostly on the European Plate, covering an area including the  
Moldanubian Variscan domain, the Bohemian Massif and the Western and Eastern Alps (2800 kg/m<sup>3</sup>). The central Alps and  
the western Po Basin are also grouped as a region of similar density (2950 kg/m<sup>3</sup>). As with the upper crust, the lower crust  
beneath the Adriatic Sea is split roughly North (2750 kg/m<sup>3</sup>) to South (3040 kg/m<sup>3</sup>) with a denser domain in the south. Lower  
crustal densities on the European and Adriatic plates have been modelled as low as 2800 kg/m<sup>3</sup> and 2750 kg/m<sup>3</sup> respectively  
205 and although necessary to resolve the gravity anomaly, these values are more similar to upper crustal density values. The other  
density domains in the lower crust of the region have values that would be expected for this depth level.

Figure 5 show the depths to the surfaces of the Moho and LAB utilised in this work. The Moho can be seen to be shallowest  
below the Ligurian Sea (20 km) but also shallow at the Ivrea body (22.5 km) and below the Upper Rhine Graben (25 km). It  
reaches its deepest point in the crustal root of the Alps at 55 km. From the gravity modelling process it was found necessary  
210 to have variation in the density of the lithospheric mantle and that the regions of different density correspond to different  
thicknesses of the lithosphere (Geissler, 2010). Broadly the lithosphere is thinnest and least dense in the North-West of the  
region (70 km and 3305 kg/m<sup>3</sup>) whilst being thickest and densest in the South-East (140 km and 3335 kg/m<sup>3</sup>) below the  
Adriatic Sea. The shallowing of the LAB below the Alps can be seen to correspond to the boundary between the Austro Alpine  
and Helvetic/Penninic Alps.

215 The full extent of the observed gravity of the modelled region is visible in Fig. 2 and the calculated gravity response is visible  
in Fig. 6. The residual anomaly of the generated model can also be seen in Fig. 6 demonstrating the close match achieved by  
the generated structural model. Almost all of the modelled area reproduces the observed gravity to  $\pm 25$  mGal with the  
exception of a couple of isolated regions where the misfit between observed and calculated gravity slightly exceeds that.

The thickness and average density of the modelled crust throughout the region are shown in Fig. 7. The thickness of the entire  
220 crust is calculated as the difference between the top surface of the upper crust and the top surface of the lithospheric mantle  
from the model. The lateral variation in average density is calculated as a weighted average taken from the thicknesses and  
densities of the upper crust and the lower crust at every point in the model.

Overall the crust can be seen to be thicker and less dense on average on the European plate (27.5 km and 2750 kg/m<sup>3</sup>) compared  
to the Adriatic (22.5 km and 2850 kg/m<sup>3</sup>). The thickest crust is found in the crustal root of the Central Alps at around 55 km  
225 thick. Areas of thinned crust are found below the sedimentary depocentres of the Po Basin and the Upper Rhine Graben, which  
can additionally be seen extending South and West of its surface location, however the crust does not appear significantly  
thinned beneath the Molasse Basin. Whilst the Adriatic crust is denser on average than the European crust it has more extreme  
density variations within it, such as a modelled low density crust in the North of the Adriatic indenter that coincides with the



230 **Veneto-Friuli plain** (2700 kg/m<sup>3</sup>), immediately adjacent to much denser crust lying to the South below the Adriatic Sea (2900 kg/m<sup>3</sup>).

Density contrasts within the crust correlate spatially with the locations of some Alpine zone boundaries as defined in the literature (Schmid et al., 1989; Schmid et al., 2004). The Briançonnais terrain can be seen as a higher density block contrasting with the rest of the zones that surround it and the Southern Alps can also be seen as a dense block, with its borders to the Briançonnais terrain and the Austro-Alpine zone clearly defined in the East of the modelled region. The Tauern window can also be seen clearly as a low density anomaly within the Austro-Alpine zone.

235 Figure 8 also shows the thickness and average density of the modelled crust, but additionally shows their correspondence with seismicity and deformation. The thickness of the crust is overlain with present day vertical displacement rates (Sternai et al., 2019) in Fig. 8a and the average density of the crust is overlain with present day horizontal surface strain distribution (Sánchez et al., 2018), seismic events of a moment magnitude of 6 or larger (Fäh et al., 2011; Stucchi et al., 2012; Grünthal et al., 2013) and the location of modelled upper crust domain boundaries in Fig. 8b, so that relationships between crustal features and deformation and seismicity can be interrogated.

240 Within the Alps a strong correlation exists between the thickness of the crust and vertical displacement rates at the surface. Regions of modelled thickened crust correspond to high positive rates of vertical displacement, such as within the Alps. Regions of thinned crust, such as in the Po Basin and the Upper Rhine Graben, were found to correspond to negative vertical displacements. Differing rates of vertical displacement can also be observed in the Western Molasse and Eastern Molasse Basin, with the west uplifting and the east subsiding. The transition between these two behaviours in the Molasse Basin corresponds to the boundary of the modelled density domain boundaries in the sedimentary and upper crustal layers, separating the denser eastern region of the basin and the less dense western portion of the basin.

245 ~~All seismic events and surface strain distribution displayed in Fig. 8b correspond to changes in density of the crust in the model.~~ Regions with a pronounced change in the density of the crust such as at the edges of the Briançonnais terrain and low density block in the north of the Adriatic Indenter are coincident with seismic events. Whilst not every seismic event corresponds to a contrast in the average density of the crust, they all correspond to the location of density domain boundaries within the upper crust as defined in the generated model. Horizontal surface strain distribution also corresponds to the location of density domain boundaries within the upper crust as defined in the model, with the direction of maximum horizontal strain 255 predominantly perpendicular to the domain boundaries.

## 5 Discussion

Differing methods of classifying the Alpine zones have been adopted over time, however the results presented here would support works that utilise tectonic reconstructions and constrain zones based on the plate the crust originated from (e.g. Schmid et al., 2004). Crust derived from different terrains could potentially be assumed to have differing properties such as density, and from the model produced in this work that is found to be the case. From the results, correlation can be observed between 260 zones of different density in the model and Alpine zones as defined by tectonic reconstructions and paleogeography, such as



the dense **Briançonnais Terrain** and Southern Alps and the less dense **Tauern Window**. As no density domain geometries were pre-defined during the modelling stage, the correlation of these domains within the generated model to known features adds validity to the generated model.

265 Additionally, Alpine zones of Adriatic provenance were found in general to be denser and those of European provenance to be less dense, a trend also noted in the present day densities of the Adriatic and European crusts, potentially indicating that prior to orogenesis this was also the case. ~~Adriatic continental crust derived~~ Alpine zones such as the Austro-Alpine and Southern Alps appear denser in general than the European continental crust derived Helvetic zone and **Tauern window**. The **Briançonnais terrain** derives from neither Europe nor Adria and as such appears ~~in the results of this work, distinct from both,~~

270 as the region of highest density in the modelled area. These observations are consistent with the interpretation that the provenance of crust within the Alps can potentially be indicated by its properties, such as density, implying that as the Alpine zones were emplaced at different times during orogenesis, the respective plates prior to orogenesis must have had similar crustal properties to the present day.

Regions in the generated model exist with similar provenance and differing densities, indicating that factors other than the

275 provenance of zones also influence their densities. This is exemplified by the Helvetic and Penninic Alps, both deriving from the European plate, ~~possessing a~~ boundary between them ~~that is clearly visible as~~ an average crustal density contrast. Additionally, some expected boundaries between crusts of different provenances ~~within the generated model~~ are obscured by other elements of the model. The transition from the European, Helvetic and Penninic, to Adriatic Austro Alpine units corresponds to the thickest area of the crustal root, where lower crust percentages are much higher than upper crust, creating

280 a region of high density crust in the model that masks the transition from European to Adriatic crust when looking at the average densities of the crust.

Correlation between present day horizontal surface deformation and large seismic events with density contrasts within the crust of the generated model would suggest the localisation of deformation along these features. Previous works have also shown correspondence between the localisation of seismicity at density contrasts within the crust such as at crustal block

285 boundaries (Dentith and Featherstone, 2003), providing further validity to the model generated in this work.

All large seismic events in the region correspond to the modelled location of upper crustal density domain boundaries, however they do not all correlate to contrasts in the average density of the crust, ~~potentially indicating~~ that within the Alps upper crustal density contrasts are a more likely location for the localisation of seismicity than ~~in the~~ lower crust. Observations of the occurrence of seismicity at depth within the Alps have shown that it is predominantly present within the upper crust (Wiemer, et al., 2017), supporting interpretations made from the derived model. However, regions exist within the model that have both

290 an average crustal density contrast and an upper crustal density domain boundary that have no seismic events, indicating that there are additional controlling factors to the localization of seismicity.

Observations of the correlation between positive vertical displacement at the surface (Sternai et al., 2019) and thickened crust within the modelled region, and negative vertical displacement and thinned crust also strengthen the validity of the el,

295 with his behaviour expected due to isostasy. ~~From the thickness of the crust it can also be seen that it~~ is significantly thinned



beneath the Po Basin of the southern foreland and not in the Molasse Basin of the northern foreland, explaining the discrepancy in deposited sediment thicknesses noted prior. This could also indicate different driving mechanisms for the formation of either basin, with the Molasse Basin potentially lacking significant subsidence due to extension, forming predominantly through flexural means, and the Po Basin forming through both flexural and active extensional processes.

300 The results presented in this work indicate crustal properties that would support observations from previous works into the dynamics of the region. Whilst correlation can be observed between vertical displacement at the surface and thickened or thinned crust, some regions such as the Molasse Basin feature a crust of similar thickness throughout but also feature a change in the polarity of surface vertical motion. The crustal densities of the model generated here would support this change however, with the transition occurring at the boundary of a density domains in the crust and the denser eastern portion exhibiting subsidence and the less dense western portion exhibiting uplift.

Previous works into the dynamics of the Adriatic plate, show that it acts as a more rigid indenter than the European plate as it moves northwards rotating counter-clockwise into it (Nocquet and Calais, 2004; Vrabec and Fodor, 2006). Results of the generated model show the Adriatic crust is denser than the European crust and seismic velocities are also observed to be higher in the Adriatic crust than the European crust (IESG, 1978; IESG & ETH Zuerich, 1981; Ströbenreuther, 1982; Mechie et al 310 1983; Zucca 1984; Gajewski & Prodehl 1985; Deichmann et al, 1986; Gajewski et al 1987; Gajewski & Prodehl 1987; Yan and Mechie 1989; Zeis et al 1990; Aichroth et al 1992; Guterch et al 1994; Ye et al 1995; Scarascia and Cassinis, 1997; Enderle et al 1998; Bleibinhaus & Gebrande, 2006; Brueckl et al., 2007). Higher densities and velocities indicate a more mafic lithology for these domains potentially suggesting that it may be stronger than the European crust. The properties of the plates as modelled here would suggest that in the converging Eastern Alps the denser Adriatic crust would subduct under the European crust which fits with the subduction polarity identified from teleseismic tomographic work in the region (Lippitsch et al., 2003) and high-resolution receiver function analysis (Hetényi et al., 2018).

Although correlations are noted between lateral variation in density distribution in the crust and observations such as plate dynamics and the localization of seismicity and deformation, the causes of these observations can not necessarily be constrained. Planned future modelling work will look closer at the features of the crust by creating thermal and rheological 320 models to give further explanation as to the driving forces behind the observed correlations, potentially helping to better explain trends noted in this work. Work is also progressing on constraining deeper structures in the region, such as the mantle, allowing for better constraints on crustal features in the future.

Although the generated model fits the observed gravity well across almost all of the modelled region, it represents a simplified version of the geology below the surface that is not able to account for all the complexity of the real world equivalent and as such, inaccuracies within the generated model exist. Additionally, whilst the location of density domains in the generated model remains a non-unique solution, efforts were made to minimise errors by using seismic data and indications from previous modelling work to constrain the densities within each layer and density domain boundaries. Whilst these uncertainties cannot 325 fully be accounted for, by only dealing with features and trends appropriate to the scale of the modelling work, they are severely



330 mitigated. At the scale of the Alps and their forelands as described in this work, irrespective of localised changes to surface heights or densities, the overall trends identified ~~in this work~~ would not be altered.

## 6 Conclusion

By creating the first gravity constrained, 3D, structural and density model of the lithosphere focused on the Alps and their respective forelands, insights were gained into the distribution of densities at depth within the crust. The findings suggest that the present day Adriatic crust is both thinner (22.5 km) and denser (2800 kg/m<sup>3</sup>) than the European crust (27.5km, 2750 kg/m<sup>3</sup>). Crust derived from different terrains was also found to have significantly different densities with Alpine zones of Adriatic provenance. The Austro-Alpine and Southern Alps were found to be denser and those of European provenance such as the Helvetic Zone and Tauern Window to be less dense, indicating the respective plates prior to orogenesis may be assumed to have had similar crustal properties to the present day.

340 ~~The model generated reproduced~~ a good fit to the observed gravity ~~field in the region~~ with maximum misfits of around  $\pm 25$  mgal across the whole region and was further validated by density domains defined in the model corresponding to known tectonic features, seismicity corresponding to **crustal density contrasts** and surface vertical displacements corresponding to crustal thicknesses. The causes of these observations and correlations ~~are unable to~~ be explained solely from the results of this work, therefore planned future modelling work will generate thermal and rheological models to give further insight into the crustal architecture of the region as well the causes of the localization of deformation and seismicity ~~within the region~~.

345

## Author Contributions

Hans-Jürgen Götze and Jörg Ebbing contributed pre-existing gravity models from the region and advised on the gravity modelling workflow and utilisation of the software used to carry it out. György Hetényi contributed seismic data for the work and advised on the interpretation of the crust and Moho in the Eastern Alps. Magdalena Scheck-Wenderoth advised on the entire workflow and the interpretation of results. Cameron Spooner carried out the modelling work and prepared the manuscript with contributions from all co-authors.

350

## References

- Aichroth, B., Prodehl, C. and Thybo, H.: Crustal structure along the Central Segment of the EGT from seismic-refraction studies. *Tectonophysics*, 207(1-2), pp.43-64, [https://doi.org/10.1016/0040-1951\(92\)90471-h](https://doi.org/10.1016/0040-1951(92)90471-h), 1992.
- 355 - Amante, C. and Eakins, B. W.: ETOPO1 1 Arc-Minute Global Relief Model: Procedures, Data Sources and Analysis. NOAA Technical Memorandum NESDIS NGDC-24, National Geophysical Data Center, NOAA, <https://doi.org/10.1594/PANGAEA.769615>, 2009.



- Babuška, V. and Plomerová, J.: The lithosphere in central Europe—seismological and petrological aspects. *Tectonophysics*, 207(1-2), pp.141-163, [https://doi.org/10.1016/0040-1951\(92\)90475-1](https://doi.org/10.1016/0040-1951(92)90475-1), 1992.
- 360 - Bleibinhaus, F. and Gebrande, H.: Crustal structure of the Eastern Alps along the TRANSALP profile from wide-angle seismic tomography. *Tectonophysics*, 414(1-4), pp.51-69, <https://doi.org/10.1016/j.tecto.2005.10.028>, 2006.
- Brocher, T.: Empirical Relations between Elastic Wavespeeds and Density in the Earth's Crust. *Bulletin of the Seismological Society of America*, 95(6), pp.2081-2092, <https://doi.org/10.1785/0120050077>, 2005.
- Brückl, E., Bleibinhaus, F., Gosar, A., Grad, M., Guterch, A., Hrubcová, P., Keller, G., Majdański, M., Šumanovac, F., Tiira, T., Yliniemi, J., Hegedűs, E. and Thybo, H.: Crustal structure due to collisional and escape tectonics in the Eastern Alps region based on profiles Alp01 and Alp02 from the ALP 2002 seismic experiment. *Journal of Geophysical Research*, 112(B6), <https://doi.org/10.1029/2006jb004687>, 2007.
- 365 - Deichmann, N., Ansorge, J. and Mueller, S.: Crustal structure of the Southern Alps beneath the intersection with the European Geotraverse. *Tectonophysics*, 126(1), pp.57-83, [https://doi.org/10.1016/0040-1951\(86\)90220-9](https://doi.org/10.1016/0040-1951(86)90220-9), 1986.
- 370 - Dentith, M. and Featherstone, W.: Controls on intra-plate seismicity in southwestern Australia. *Tectonophysics*, 376(3-4), pp.167-184, <https://doi.org/10.1016/j.tecto.2003.10.002>, 2003.
- Deutsch, C.: 2D Gravity Modeling and Evaluation of the Lithospheric Structure of the Alpine Collision Zone along the TRANSALP Profile. Masters Thesis. Freien Universität Berlin, 2014.
- Dèzes, P., Schmid, S. and Ziegler, P.: Evolution of the European Cenozoic Rift System: interaction of the Alpine and Pyrenean orogens with their foreland lithosphere. *Tectonophysics*, 389(1-2), pp.1-33, <https://doi.org/10.1016/j.tecto.2004.06.011>, 2004.
- 375 - Ebbing, J.: 3-D Dichteverteilung und isostatisches Verhalten der Lithosphäre in den Ostalpen. Ph.D Thesis. Freien Universität Berlin, 2002.
- Enderle, U., Schuster, K., Prodehl, C., Schulze, A. and Bribach, J.: The refraction seismic experiment GRANU95 in the Saxothuringian belt, southeastern Germany. *Geophysical Journal International*, 133(2), pp.245-259, <https://doi.org/10.1046/j.1365-246x.1998.00462.x>, 1998.
- 380 - Fäh, D., Giardini, D., Kästli, P., Deichmann, N., Gisler, M., Schwarz-Zanetti, G., Alvarez-Rubio, S., Sellami, S., Edwards, B., Allmann, B., Bethmann, F., Wössner, J., Gassner-Stamm, G., Fritsche, S., Eberhard, D.: ECOS-09 Earthquake Catalogue of Switzerland Release 2011 Report and Database. Public catalogue, 17. 4. 2011. Swiss Seismological Service ETH Zurich, Report SED/RISK/R/001/20110417, 2011.
- 385 - Förste, C., Bruinsma, S. L., Abrikosov, O., Lemoine, J. M., Marty, J. C., Flechtner, F., Balmino, G., Barthelmes, F., Biancale, R.: EIGEN-6C4 The latest combined global gravity field model including GOCE data up to degree and order 2190 of GFZ Potsdam and GRGS Toulouse. GFZ Data Services, <http://doi.org/10.5880/icgem.2015.1>, 2014.
- Franke, W.: The mid-European segment of the Variscides: tectonostratigraphic units, terrane boundaries and plate tectonic evolution. *Geological Society, London, Special Publications*, 179(1), pp.35-61, <https://doi.org/10.1144/gsl.sp.2000.179.01.05>, 2000.
- 390



- Freymark, J., Sippel, J., Scheck-Wenderoth, M., Bär, K., Stiller, M., Fritsche, J. and Kracht, M.: The deep thermal field of the Upper Rhine Graben. *Tectonophysics*, 694, pp.114-129, <https://doi.org/10.1016/j.tecto.2016.11.013>, 2017.
- Frisch, W.: Tectonic progradation and plate tectonic evolution of the Alps. *Tectonophysics*, 60(3-4), pp.121-139, 395 [https://doi.org/10.1016/0040-1951\(79\)90155-0](https://doi.org/10.1016/0040-1951(79)90155-0), 1979.
- Gajewski, D. and Prodehl, C.: Crustal structure beneath the Swabian Jura, SW Germany, from seismic refraction investigations. *Journal of Geophysics*, 56, pp.69-80, 1985.
- Gajewski, D. and Prodehl, C.: Seismic refraction investigation of the Black Forest. *Tectonophysics*, 142(1), pp.27-48, 400 [https://doi.org/10.1016/0040-1951\(87\)90293-9](https://doi.org/10.1016/0040-1951(87)90293-9), 1987.
- Gajewski, D., Holbrook, W. and Prodehl, C.: A three-dimensional crustal model of southwest Germany derived from seismic refraction data. *Tectonophysics*, 142(1), pp.49-70, [https://doi.org/10.1016/0040-1951\(87\)90294-0](https://doi.org/10.1016/0040-1951(87)90294-0), 1987.
- Geissler, W., Sodoudi, F. and Kind, R.: Thickness of the central and eastern European lithosphere as seen by S receiver functions. *Geophysical Journal International*, <https://doi.org/10.1111/j.1365-246x.2010.04548.x>, 2010.
- Grünthal, G., Wahlström, R. and Stromeyer, D.: The SHARE European Earthquake Catalogue (SHEEC) for the time period 405 1900–2006 and its comparison to the European-Mediterranean Earthquake Catalogue (EMEC). *Journal of Seismology*, 17(4), pp.1339-1344, <https://doi.org/10.1007/s10950-013-9379-y>, 2013.
- Guterch, A., Grad, M., Janik, T., Materzok, R., Luosto, U., Yliniemi, J., Lück, E., Schulze, A. and Förste, K.: Crustal structure of the transition zone between Precambrian and Variscan Europe from new seismic data along LT-7 profile (NW Poland and eastern Germany). *C. R. Acad. Sci. Paris*, 319, pp.1489–1496, 1994.
- 410 - Handy, M., M. Schmid, S., Bousquet, R., Kissling, E. and Bernoulli, D.: Reconciling plate-tectonic reconstructions of Alpine Tethys with the geological–geophysical record of spreading and subduction in the Alps. *Earth-Science Reviews*, 102(3-4), pp.121-158, <https://doi.org/10.1016/j.earscirev.2010.06.002>, 2010.
- Hetényi, G., Plomerová, J., Bianchi, I., Kampfová Exnerová, H., Bokelmann, G., Handy, M. and Babuška, V.: From mountain summits to roots: Crustal structure of the Eastern Alps and Bohemian Massif along longitude 13.3°E. *Tectonophysics*, 744, 415 pp.239-255, <https://doi.org/10.1016/j.tecto.2018.07.001>, 2018.
- IESG: Alp 75 d-h. *Boll. di Geofisica Teorica ed Applicata*, 20, pp.287-302, 1978.
- IESG and ETH: Südalp 77 b-d. *Boll. di Geofisica Teorica ed Applicata*, 23, pp.297-330, 1981.
- Ince, E., Barthelmes, F., Reißland, S., Elger, K., Förste, C., Flechtner, F. and Schuh, H.: ICGEM - 15 years of successful collection and distribution of global gravitational models, associated services and future plans. *Earth System Science Data* 420 *Discussions*, pp.1-61, <https://doi.org/10.5194/essd-11-647-2019>, 2019.
- Lippitsch, R., Kissling, E. and Ansorge, J.: Upper mantle structure beneath the Alpine orogen from high-resolution teleseismic tomography. *Journal of Geophysical Research*, 108(B8), <https://doi.org/10.1029/2002jb002016>, 2003.
- Lowe, M. Sensitivity study on separation of crustal and mantle contribution to the Alpine gravity field. Masters Thesis. Christian-Albrechts-Universität Kiel. ~~Manuscript in preparation~~, 2019.



- 425 - Mechie, J., Prodehl, C. and Fuchs, K.: Seismic refraction investigations of crust and uppermost mantle structure beneath the Rhenish Massif. *Tectonophysics*, 118(1-2), pp.159-160, [https://doi.org/10.1016/0040-1951\(85\)90165-9](https://doi.org/10.1016/0040-1951(85)90165-9), 1985.
- Molinari, I. and Morelli, A.: EPcrust: a reference crustal model for the European Plate. *Geophysical Journal International*, 185(1), pp.352-364, <https://doi.org/10.1111/j.1365-246x.2011.04940.x>, 2011.
- Molinari, I., Argnani, A., Morelli, A. and Basini, P.: Development and Testing of a 3D Seismic Velocity Model of the Po  
430 Plain Sedimentary Basin, Italy. *Bulletin of the Seismological Society of America*, 105(2A), pp.753-764, <https://doi.org/10.1785/0120140204>, 2015.
- Nocquet, J. and Calais, E.: Geodetic Measurements of Crustal Deformation in the Western Mediterranean and Europe. *Pure and Applied Geophysics*, 161(3), pp.661-681, <https://doi.org/10.1007/s00024-003-2468-z>, 2004.
- Pistone, M., Müntener, O., Ziberna, L., Hetényi, G. and Zanetti, A.: Report on the ICDP workshop DIVE (Drilling the Ivrea-  
435 Verbano zone). *Scientific Drilling*, 23, pp.47-56, <https://doi.org/10.5194/sd-23-47-2017>, 2017.
- Przybycin, A., Scheck-Wenderoth, M. and Schneider, M.: Assessment of the isostatic state and the load distribution of the European Molasse basin by means of lithospheric-scale 3D structural and 3D gravity modelling. *International Journal of Earth Sciences*, 104(5), pp.1405-1424, <https://doi.org/10.1007/s00531-014-1132-4>, 2014.
- Restivo, A., Bressan, G. and Segan, M.: Stress and strain patterns in the Venetian Prealps (north-eastern Italy) based on focal-  
440 mechanism solutions. *Bollettino di Geofisica Teorica ed Applicata*, 57(1), pp.13-30, 2016.
- Sánchez, L., Völksen, C., Sokolov, A., Arenz, H. and Seitz, F.: Present-day surface deformation of the Alpine region inferred from geodetic techniques. *Earth System Science Data*, 10(3), pp.1503-1526, <https://doi.org/10.5194/essd-10-1503-2018>, 2018.
- Scarascia, S. and Cassinis, R.: Crustal structures in the central-eastern Alpine sector: A revision of the available DSS data. *Tectonophysics*, 271(1-2), pp.157-188, [https://doi.org/10.1016/s0040-1951\(96\)00206-5](https://doi.org/10.1016/s0040-1951(96)00206-5), 1997.
- 445 - Schlumberger.: *Petrel* (2011.1.2) [Computer program], 1998.
- Schmid, S., Aebli, H., Heller, F. and Zingg, A.: The role of the Periadriatic Line in the tectonic evolution of the Alps. *Geological Society, London, Special Publications*, 45(1), pp.153-171, <https://doi.org/10.1144/gsl.sp.1989.045.01.08>, 1989.
- Schmid, S., Fügenschuh, B., Kissling, E. and Schuster, R. (2004). Tectonic map and overall architecture of the Alpine orogen. *Eclogae Geologicae Helvetiae*, 97(1), pp.93-117, <https://doi.org/10.1007/s00015-004-1113-x>, 2004.
- 450 - Schmidt, S., Götze, H. J., Fichler, C., Ebbing, J., Alvers, M. R.: 3D Gravity, FTG and magnetic modeling: the new IGMAS + software. *Geoinformatik 2010*, 2010.
- Sternai, P., Sue, C., Husson, L., Serpelloni, E., Becker, T., Willett, S., Faccenna, C., Di Giulio, A., Spada, G., Jolivet, L., Valla, P., Petit, C., Nocquet, J., Walpersdorf, A. and Castellort, S.: Present-day uplift of the European Alps: Evaluating mechanisms and models of their relative contributions. *Earth-Science Reviews*, 190, pp.589-604, <https://doi.org/10.1016/j.earscirev.2019.01.005>, 2019.
- 455 - Ströbenreuther, U.: Die Struktur der Erdkruste am Südwestrand der Böhmisches Masse, abgeleitet aus refraktionsseismischen Messungen der Jahre 1970 und 1978/79. Ph.D. Thesis, Universität München, 1982.



- Stucchi, M., Rovida, A., Gomez Capera, A., Alexandre, P., Camelbeeck, T., Demircioglu, M., Gasperini, P., Kouskoua, V., Musson, R., Radulian, M., Sesetyan, K., Vilanova, S., Baumont, D., Bungum, H., Fäh, D., Lenhardt, W., Makropoulos, K.,  
460 Martinez Solares, J., Scotti, O., Živčić, M., Albin, P., Batllo, J., Papaioannou, C., Tatevossian, R., Locati, M., Meletti, C.,  
Viganò, D. and Giardini, D.: The SHARE European Earthquake Catalogue (SHEEC) 1000–1899. *Journal of Seismology*,  
17(2), pp.523-544, <https://doi.org/10.1007/s10950-012-9335-2>, 2012.
- Tesauro, M., Kaban, M. and Cloetingh, S.: EuCRUST-07: A new reference model for the European crust. *Geophysical Research Letters*, 35(5), <https://doi.org/10.1029/2007gl032244>, 2008.
- 465 - Turrini, C., Lacombe, O. and Roure, F.: Present-day 3D structural model of the Po Valley basin, Northern Italy. *Marine and Petroleum Geology*, 56, pp.266-289, <https://doi.org/10.1016/j.marpetgeo.2014.02.006>, 2014.
- Vrabec M, Fodor L.: Late Cenozoic tectonics of Slovenia: structural styles at the northeastern corner of the Adriatic microplate. In: Pinter N, Grenerczy G, Weber J, Stein S, Medak D (eds) *The Adria microplate: GPS geodesy, tectonics and hazards*, vol 61: Nato Scie Series, IV, earth and environmental science, vol 61. Springer, Dordrecht, pp 151–158, 2006.
- 470 - Wiemer, S., Kraft, T., Trutnevyte, E., & Roth, P.: “ Good Practice ” Guide for Managing Induced Seismicity in Deep Geothermal Energy Projects in Switzerland, SED, Swiss Seismological Service at ETH Zürich, <https://doi.org/10.3929/ethz-b-000254161>, 2017
- Yan, Q. and Mechie, J.: A fine structural section through the crust and lower lithosphere along the axial region of the Alps. *Geophysical Journal International*, 98(3), pp.465-488, <https://doi.org/10.1111/j.1365-246x.1989.tb02284.x>, 1989.
- 475 - Ye, S., Ansorge, J., Kissling, E. and Mueller, S.: Crustal structure beneath the eastern Swiss Alps derived from seismic refraction data. *Tectonophysics*, 242(3-4), pp.199-221, [https://doi.org/10.1016/0040-1951\(94\)00209-r](https://doi.org/10.1016/0040-1951(94)00209-r), 1995.
- Zeis, S., Gajewski, D. and Prodehl, C.: Crustal structure of southern Germany from seismic refraction data. *Tectonophysics*, 176(1-2), pp.59-86, [https://doi.org/10.1016/0040-1951\(90\)90259-b](https://doi.org/10.1016/0040-1951(90)90259-b), 1990.
- Zingg, A., Handy, M., Hunziker, J. and Schmid, S.: Tectonometamorphic history of the Ivrea Zone and its relationship to the  
480 crustal evolution of the Southern Alps. *Tectonophysics*, 182(1-2), pp.169-192, [https://doi.org/10.1016/0040-1951\(90\)90349-d](https://doi.org/10.1016/0040-1951(90)90349-d), 1990.
- Zucca, J.J.: The crustal structure of the southern Rhine graben from the reinterpretation of seismic refraction data. *Journal of Geophysics - Zeitschrift für Geophysik*, 55, pp.13-22, <https://doi.org/10.23689/figeo-3178>, 1984.

485

### Figure Captions

- Figure 1. a) Topography and bathymetry from Etopo 1 (Amante and Eakins, 2009) shown across the Alpine region. Study area is indicated with a black box. Solid lines demark the boundaries of Alpine zones, dotted black lines indicate the extent of the unaccreted Adriatic plate. Key tectonic features have been labelled: URG – Upper Rhine Graben; BOH – Bohemian Massif; VOS – Vosges Massif;  
490 BLF – Black Forest Massif; MOL – Molasse Basin; AA – Austro-Alpine Zone; TW – Tauern Window; HA – Helvetic Alps; PA – Penninic Alps; SA – Southern Alps; BT – Briançonnais Terrain; IVR – Ivrea Body; PO – Po Basin; APP – Apennine Plate. b) Input data source



495 extents: Upper Rhine Graben gravity constrained model (Freyermark et al., 2017); Molasse Basin gravity constrained model (Przybycin et al., 2015); TRANSALP gravity constrained model (Ebbing, 2002); Po basin seismically constrained models (Turini et al., 2014; Molinari et al., 2015); and Seismic Sections (IESG, 1978; IESG & ETH Zuerich, 1981; Ströbenreuther, 1982; Mechie et al., 1983; Zucca, 1984; Gajewski & Prodehl, 1985; Deichmann et al., 1986; Gajewski et al., 1987; Gajewski & Prodehl, 1987; Yan and Mechie, 1989; Zeis et al., 1990; Aichroth et al., 1992; Guterch et al., 1994; Ye et al., 1995; Scarascia and Cassinis, 1997; Enderle et al., 1998; Bleibinhaus & Gebrande, 2006; Brueckl et al., 2007; Hetényi et al., 2018). 

- Figure 2. Observed gravity of the region. Values calculated from a spherical approximation at 6km above datum of EIGEN-6C4 global gravity model (Förste et al., 2014). Locations of key tectonic features are overlain (abbreviations shown in Fig. 1a caption). 

500 - Figure 3. Cross sections through generated model showing thickness of model layers. Location is marked in Fig. 1a. Lithospheric mantle layer is shown in red, lower crust is shown in grey, upper crust is shown in brown, consolidated sediments are shown in blue and unconsolidated sediments are shown in yellow. In Fig. 3. a) Density domains within each layer are shown as a change of shade and the densities of each domain are labelled. The observed and calculated ~~response of the gravity~~ throughout the cross section are shown. Fig. b) is scaled to show the thicknesses of all layers down to the ~~aesthenospheric~~ mantle, shown in orange.

505 - Figure 4. Thickness of a) unconsolidated sediments, b) consolidated sediments, c) the upper crust and d) the lower crust across the modelled area. Density domains required within the layer are overlain in white, layer numbers are shown in white and correspond to Table 1. Locations of key tectonic features are overlain (abbreviations shown in Fig. 1a caption).

- Figure 5. a) Depth to ~~top surface of~~ the Moho across the modelled area. Density domains required within the layer are overlain in white, layer numbers are shown in white and correspond to Table 1. b) Depth to ~~top surface of~~ the LAB from Geissler (2010) across the modelled area. Solid lines demark the boundaries of Alpine zones, the dotted black lines indicate the extent of the unaccreted Adriatic plate. Locations of key tectonic features are overlain for both figures (abbreviations shown in Fig. 1a caption).

515 - Figure 6. a) Calculated gravity ~~of the region~~ at 6km above the datum resulting from the final structural and density model ~~produced in this work~~. b) Residual gravity after calculated gravity has been subtracted from observed gravity ~~in the region~~. Solid lines demark the boundaries of Alpine zones, dotted black lines indicate the extent of the unaccreted Adriatic plate. Locations of key tectonic features are overlain for both figures (abbreviations shown in Fig. 1a caption).

- Figure 7. a) Thickness and b) average density of the entire crust across the modelled area. Solid lines demark the boundaries of Alpine zones, the dotted black lines indicate the extent of the unaccreted Adriatic plate. Locations of key tectonic features are overlain (abbreviations shown in Fig. 1a caption).

520 - Figure 8. a) Thickness of the crust across the modelled area overlain with vertical displacement rates (Sternai et al., 2019). Dotted black lines indicate isolines ~~relating to~~ the vertical displacement rates in mm/a. Regions where the overlain data was not available have been whited out. Locations of key tectonic features are overlain (abbreviations shown in Fig. 1a caption). b) Average density of the crust across the modelled area overlain with geodetically derived horizontal surface strain distribution ~~from~~ (Sánchez et al., 2018) and seismic events of a Moment Magnitude ~~over magnitude~~ 6 (Fäh et al., 2011; Stucchi et al., 2012; Grünthal et al., 2013). Stick orientation indicates orientation of maximum surface strain. Dotted black lines indicate the upper crust density domains of the final structural and density model ~~produced in this work~~. Regions where the overlain data was not available have been whited out. Locations of key tectonic features are overlain  
525 (abbreviations shown in Fig. 1a caption).

## Tables



Table 1 -

Unit	Mean Density indicated by P Wave Velocities (Kg/m3)	Density Used in Final Model (Kg/m3)
1. Unconsolidated Sediments	2530	2450
2. Unconsolidated Sediments – East Molasse	2540	2470
3. Unconsolidated Sediments - Po	2610	2470
4. Consolidated Sediments	2680	2670
5. Consolidated Sediments – East Molasse	2670	2680
6. Consolidated Sediments - Po	2700	2700
7. Upper Crust – Saxothuringia	2690	2670
8. Upper Crust – Moldanubia	2710	2700
9. Upper Crust – Bohemia	2720	2740
10. Upper Crust – Vosges and Black Forest	2690	2660
11. Upper Crust – East Molasse	2720	2720
12. Upper Crust – East Alps	2740	2740
13. Upper Crust – West Alps	2740	2670
14. Upper Crust – Po	2740	2730
15. Upper Crust – North East Adria	2780	2660



16. Upper Crust – Ivrea	-	2790
17. Upper Crust – East Adria	2780	2700
18. Upper Crust – Apennine	2770	2720
19. Lower Crust – Saxothuringia	2900	2920
20. Lower Crust – Europe	2890	2800
21. Lower Crust – Alps	2880	2950
22. Lower Crust – Ivrea	-	3100
23. Lower Crust – Northern Adria	2990	2750
24. Lower Crust – East Adria	2950	3040
25. Lithospheric Mantle – Less Dense	3340	3305
26. Lithospheric Mantle – More Dense	3260	3335
Water	-	1025
Asthenospheric Mantle	-	3320

530

#### Table Captions

- Table 1. The density of each domain in the model indicated by converting from its mean P wave velocity using the empirical relationship detailed in Brocher (2005) and the density of all domains used in the final model of the region found to best reproduce the indications of both the seismic data sources and the gravity field. Locations of each density domain can be found in Fig. 4.

535



Figure 1

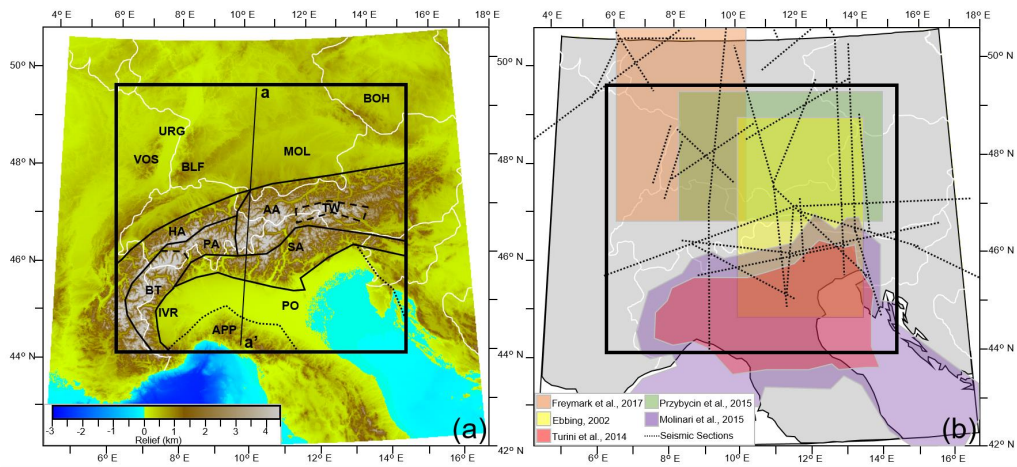




Figure 2

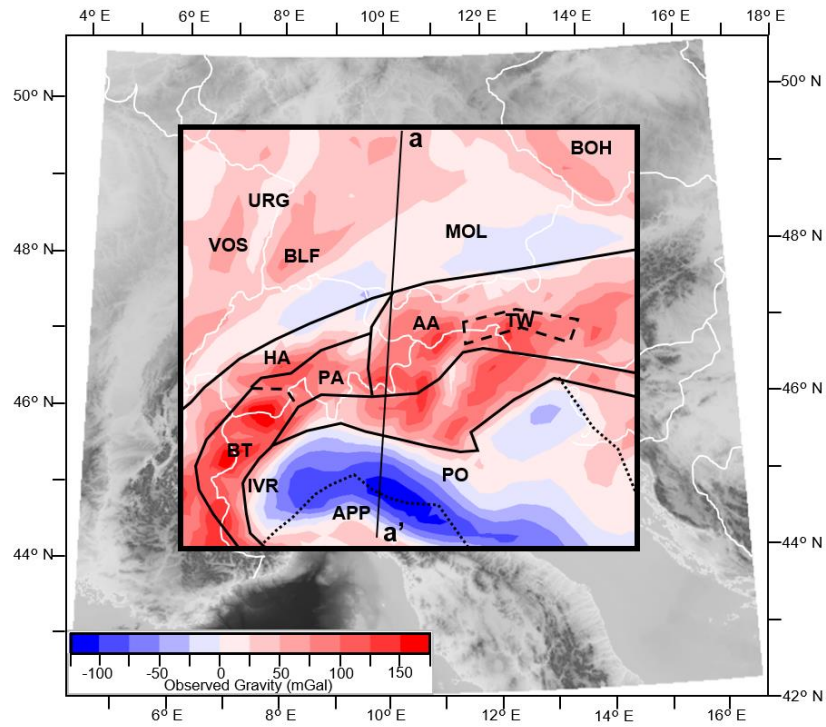




Figure 3

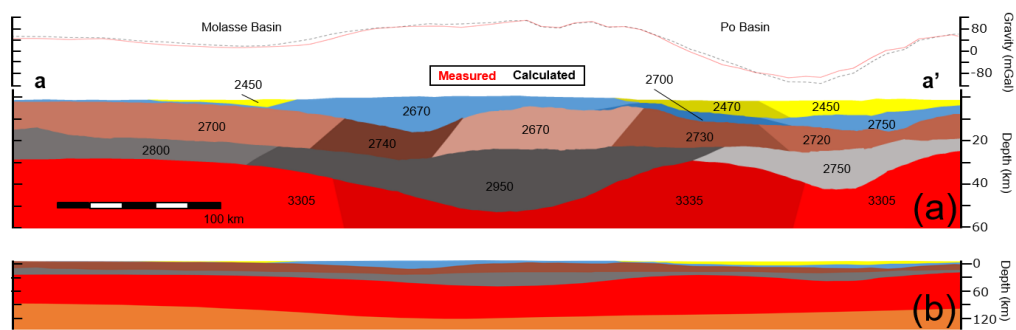




Figure 4

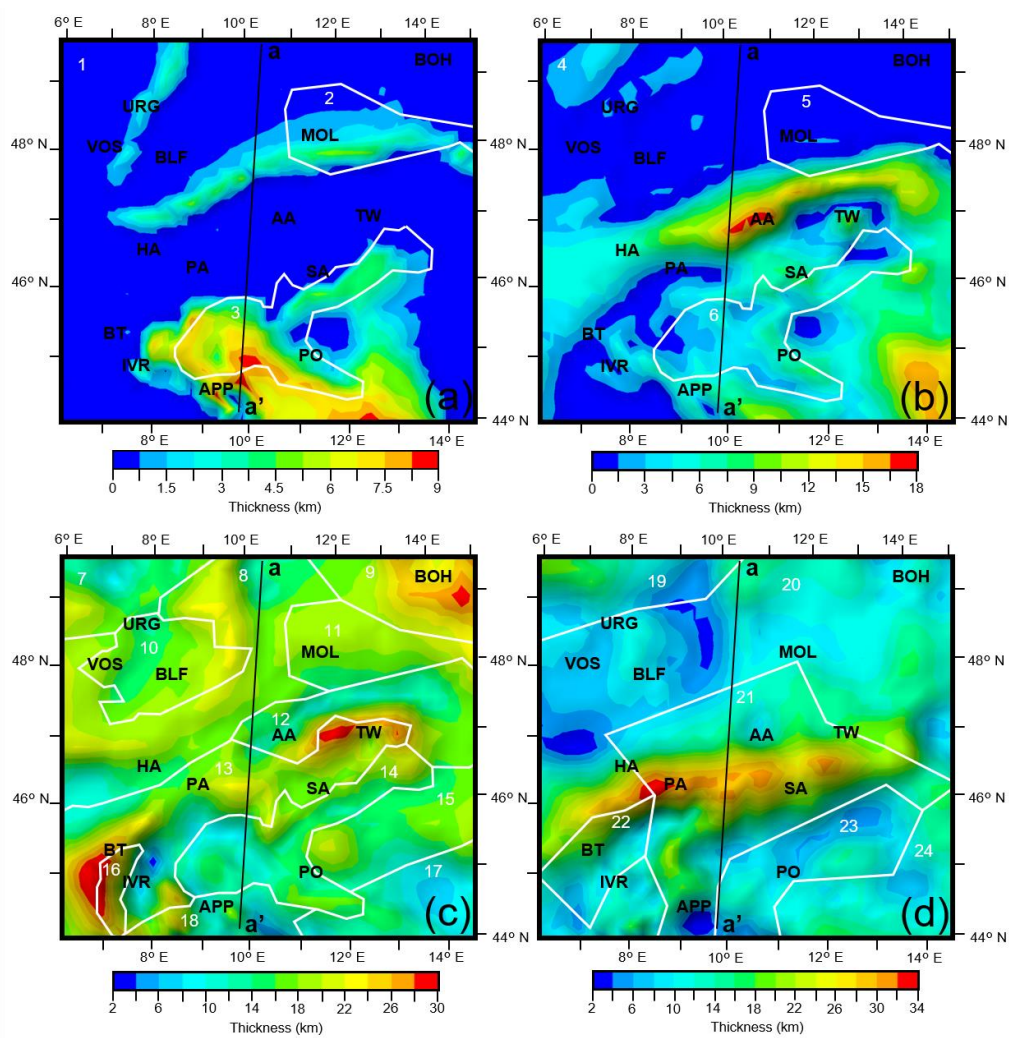




Figure 5

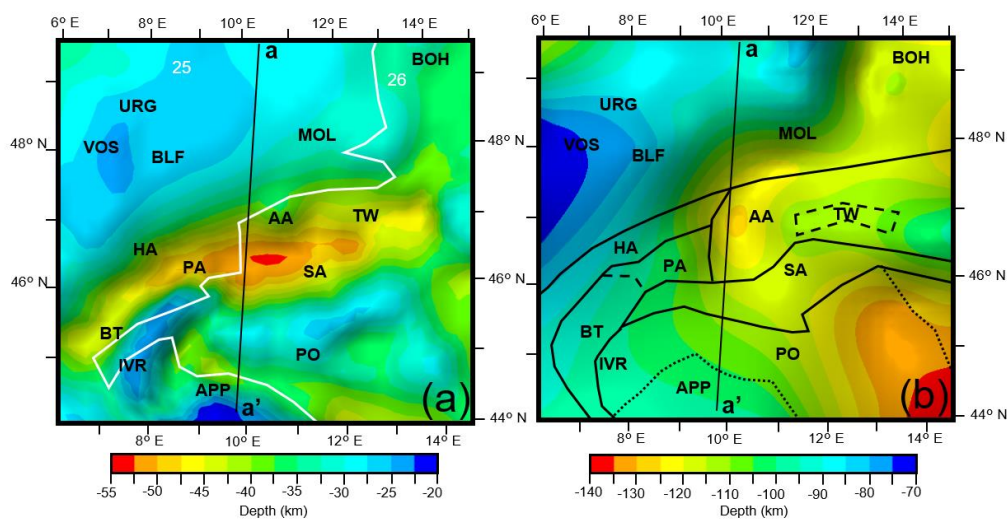




Figure 6

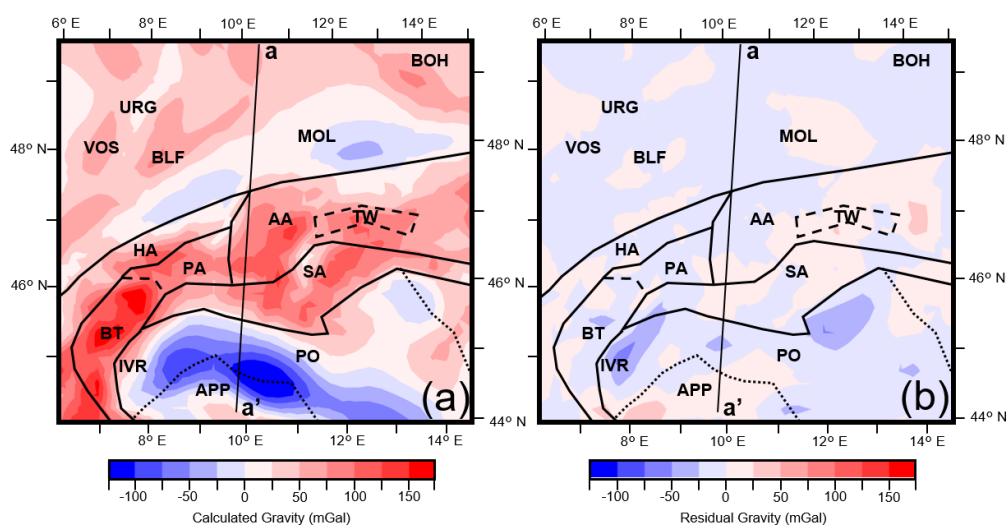




Figure 7

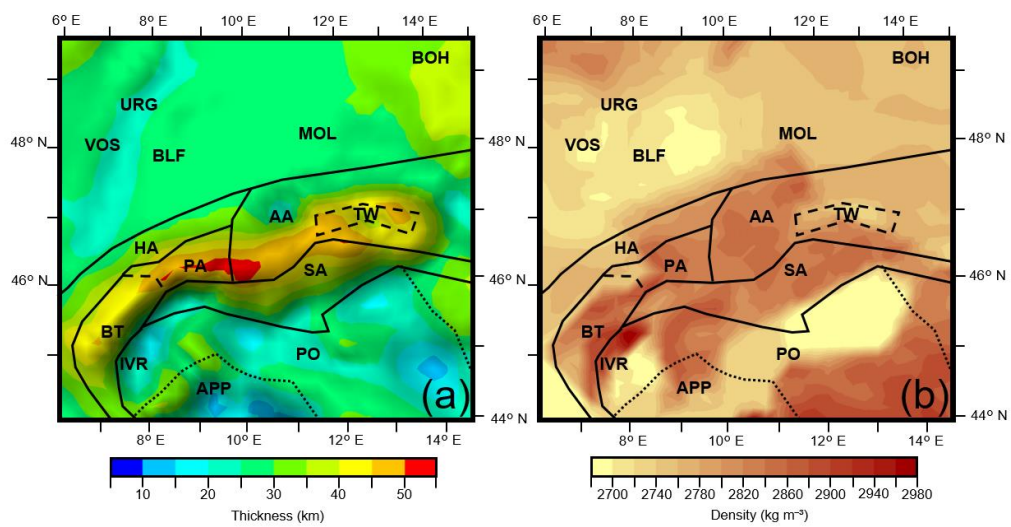




Figure 8

